The *MicroRNA390/TRANS-ACTING SHORT INTERFERING RNA3* Module Mediates Lateral Root Growth under Salt Stress via the Auxin Pathway[1]

Fu He,[2] Changzheng Xu,[2] Xiaokang Fu, Yun Shen, Li Guo, Mi Leng, and Keming Luo[3]

Key Laboratory of Eco-environments of Three Gorges Reservoir Region, Ministry of Education, Chongqing Key Laboratory of Transgenic Plant and Safety Control, Institute of Resources Botany, School of Life Sciences, Southwest University, Chongqing 400715, China

ORCID IDs: 0000-0001-8421-6244 (L.G.); 0000-0003-4928-7578 (K.L.)

Salt-induced developmental plasticity in a plant root system strongly depends on auxin signaling. However, the molecular events underlying this process are poorly understood. *MicroRNA390* (*miR390*), *trans-actin small interfering RNA*s (*tasiRNA*s), and *AUXIN RESPONSE FACTORs* (*ARFs*) form a regulatory module involved in controlling lateral root (LR) growth. Here, we found that *miR390* expression was strongly induced by exposure to salt during LR formation in poplar (*Populus* spp.) plants. *miR390* overexpression stimulated LR development and increased salt tolerance, whereas *miR390* knockdown caused by a short tandem target mimic repressed LR growth and compromised salt resistance. *ARF3.1*, *ARF3.2*, and *ARF4* expression was inhibited significantly by the presence of salt, and transcript abundance was decreased dramatically in the *miR390*-overexpressing line but increased in the *miR390*-knockdown line. Constitutive expression of *ARF4m* harboring mutated *trans-acting small interfering ARF*-binding sites removed the salt resistance of the *miR390* overexpressors. *miR390* positively regulated auxin signaling in LRs subjected to salt, but *ARF4* inhibited auxin signaling. Salinity stabilized the poplar Aux/IAA repressor INDOLE-3-ACETIC ACID17.1, and overexpression of an auxin/salt-resistant form of this repressor suppressed LR growth in *miR390*-overexpressing and *ARF4*-RNA interfering lines in the presence of salt. Thus, the *miR390/TAS3/ARFs* module is a key regulator, via modulating the auxin pathway, of LR growth in poplar subjected to salt stress.

Due to climate change and agricultural practice, increase in soil salinity is a major threat to crop yields around the world (Munns and Tester, 2008). Salt generally damages plants through osmotic stress in the rhizosphere, interfering with water and nutrient uptake and causing cells to be subjected to ionic toxicity (Hasegawa et al., 2000; Zhang and Shi, 2013). Developmental plasticity in the root system is an important strategy allowing plants to cope with environmental stresses, including salinity (Galvan-Ampudia and Testerink, 2011). Salt-induced plasticity occurs in a number of root development processes, such as primary root elongation, lateral root (LR) growth, root hair formation, and root tropism (Sun et al., 2008; Wang et al., 2008, 2009; Galvan-Ampudia et al., 2013). Relatively little is known about the genetic and molecular events underlying salt-induced root plasticity, even though morphological modifications in roots are very important to the adaptabilities of higher plants to the presence of salt.

Salt responses in plant roots require sophisticated and coordinated spatial-temporal transcriptional programs and the regulation of hormones, including auxin, abscisic acid, and GA (Duan et al., 2013; Galvan-Ampudia et al., 2013; Geng et al., 2013; Liu et al., 2015). Auxin is a well-known phytohormone that triggers root genesis and salt-induced root developmental plasticity (Kazan, 2013). Meristematic activity and root pattern formation are determined by the distal auxin maximum in Arabidopsis (*Arabidopsis thaliana*) root tips (Sabatini et al., 1999; Blilou et al., 2005), orchestrated by polar auxin transport (Palme and Gälweiler, 1999; Friml et al., 2002). Decreases in meristem size when plants suffer from salt stress inhibit root cell proliferation and elongation (West et al., 2004), and salt-restricted auxin accumulation occurs in the root tips (Liu et al., 2015). Halotropism, which allows roots to bend away from areas with high salt concentrations, requires the active redistribution of auxin in the root tips, mediated by PIN-FORMED2 (PIN2; Galvan-Ampudia et al., 2013). The sensitivity of root tissues to salt can be modified by polar auxin transport modulation and

[1]This work was supported by grants from the National Key Research and Development Program (2016YFD0600105 to K.L.), by the National Natural Science Foundation of China (31370672 to K.L. and 31500216 to C.X.), by Fundamental Research Funds for the Central Universities (XDJK2016B032 to C.X.), and by the National Undergraduate Innovation and Entrepreneurship Training Program of China (201601635021 to M.L.).

[2]These authors contributed equally to the article.

[3]Address correspondence to kemingl@swu.edu.cn.

The author responsible for distribution of materials integral to the findings presented in this article in accordance with the policy described in the Instructions for Authors (www.plantphysiol.org) is: Keming Luo (kemingl@swu.edu.cn).

K.L. and C.X. designed the research; F.H., C.X., X.F., Y.S., M.L., and L.G. performed the experiments; K.L. and C.X. analyzed the data and wrote the article.

www.plantphysiol.org/cgi/doi/10.1104/pp.17.01559

changes in the protein turnover of Aux/IAAs (a family of transcriptional repressors involved in auxin signaling; Wang et al., 2009; Liu et al., 2015). Auxin perception starts with the direct binding of auxin to its receptors TIR1 (TRANSPORT INHIBITOR RESPONSE1)/AFB (AUXIN SIGNALING F-BOX; Dharmasiri et al., 2005; Kepinski and Leyser, 2005), which are posttranscriptionally targeted by *microRNA393* (*miR393*; Si-Ammour et al., 2011). The *miR393*-dependent regulation of TIR1/AFBs is a critical checkpoint in auxin signaling, coordinating auxin signaling with root growth under saline conditions (Iglesias et al., 2014). The Salt Overly Sensitive (SOS) pathway is a well-understood module coupling salt signals with sodium homeostasis; it plays a critical role in salt-induced plastic LR development via the modulation of auxin distribution in the presence of salt (Zhao et al., 2011; Ji et al., 2013). Thus, auxin plays key roles in integrating a salt stimulus into root development programs. A comprehensive understanding of salt-induced root plasticity requires the identification of more novel components and pathways within the salt/auxin-mediated molecular framework (Galvan-Ampudia and Testerink, 2011).

miR390 is an evolutionarily conserved microRNA (miRNA) that specifically binds to and then cleaves transcripts of the noncoding *trans-acting short interfering RNA3* (*TAS3*; Allen et al., 2005). A number of molecular components involved in small interfering RNA biogenesis, including RNA-DEPENDENT RNA POLYMERASE6, SUPPRESSOR OF GENE SILENCING3, and DICER-LIKE4, allow the cleaved *TAS3* transcript fragments to produce *trans-acting small interfering RNAs* (Xie et al., 2005). The *TAS3*-derived *trans-acting small interfering RNA*s can mediate the cleavage of transcripts encoding AUXIN RESPONSE FACTOR2 (ARF2), ARF3, and ARF4, so they are also called *trans-acting small interfering* (*tasi*) *ARFs* (Marin et al., 2010). ARF proteins are key components of the auxin signaling cascade and directly control the transcription of primary auxin-responsive genes (Guilfoyle and Hagen, 2007). The *miR390/TAS3/ARFs* module is functionally diverse, regulating a number of plant development processes. The *tasiARFs* derived from *miR390*-cleaved *TAS3* transcripts are key regulators of leaf patterning, leaf polarity, leaf expansion, and developmental phase transition (Adenot et al., 2006; Fahlgren et al., 2006; Garcia et al., 2006; Yifhar et al., 2012). The *miR390/TAS3/ARFs* pathway is part of the auxin-mediated molecular network that orchestrates LR formation in Arabidopsis (Marin et al., 2010; Yoon et al., 2010). This pathway also is required for the initiation of the shoot meristem in rice (*Oryza sativa*; Nagasaki et al., 2007). In legume species, the *miR390/TAS3* pathway regulates lateral organ development and leaf margin formation (Zhou et al., 2013) and also plays an important role in root nodule symbiosis (i.e. facilitating plant-microbe interactions; De Luis et al., 2012; Li et al., 2014; Cabrera et al., 2016). The *miR390/TAS3* pathway modulates LR growth but encourages nodule development in legumes (Hobecker et al., 2017). However, it is still unclear whether the *miR390/TAS3/ARFs* module is involved in the responses of plants to abiotic stresses.

Poplar (*Populus* spp.) are fast-growing woody plants of great economical and ecological importance (Dickmann, 2006). Different poplar species and ecotypes have very different salt tolerances, allowing the *Populus* genus to be used as an ideal model when studying physiological and genetic salt acclimation strategies (Chen and Polle, 2010). A number of transcription factors, including GRAS (GIBBERELLIN-INSENSITIVE, REPRESSOR OF GAI, and SCARECROW)/SCL (SCARECROW-LIKE7), ERF (ETHYLENE RESPONSE FACTOR76), HDG (HOMEODOMAIN GLABROUS11), and WRKY70 (the homologs of which have been found to regulate stress responses in other species), have been found to participate in the transcriptional regulation of salt tolerance in poplar (Ma et al., 2010; Yao et al., 2016; Yu et al., 2016; Zhao et al., 2017). Studies of transgenic poplar indicate that the SOS pathway is involved in salt tolerance, as it is in herbaceous Arabidopsis (Tang et al., 2010; Yang et al., 2015; Ke et al., 2017). Little is known about the underlying molecular processes involved in salt tolerance in *Populus* spp. miRNAs in *Populus euphratica*, a salt-tolerant poplar species, have been comprehensively profiled, and salt-induced expression of a series of *miRNAs*, including *miR390*, occurs in root tissues (Si et al., 2014). Salt-responsive modulation of the *miR390/ARF* unit has been found in a comprehensive small RNA profiling survey of cotton (*Gossypium hirsutum*; Yin et al., 2017). Here, we determine the salt-responsive expression of *miR390* in poplar during LR formation and functionally characterize *miR390/ARF4* under saline conditions using genetically transformed poplar plants. The results indicate that the *miR390/TAS3/ARF* module, an evolutionarily conserved pathway, is involved in salt-induced LR development regulation in poplar via the auxin pathway.

RESULTS

Salt-Induced Expression of *miR390* during LR Development in Poplar

The *miR390* family in genus *Populus* has four members that, despite some rather variable flanking sequences, have a 21-bp mature sequence identical to that in Arabidopsis *miR390* (miRbase: http://www.mirbase.org; Supplemental Fig. S1A). As predicted by the RNAfold WebServer (Gruber et al., 2008), the precursors of the poplar *miR390* members form stem-loop secondary structures and generate the same mature *miRNA* (Supplemental Fig. S1B). Reverse transcription-quantitative PCR (RT-qPCR) showed that mature *miR390* is expressed throughout roots and leaves (Supplemental Fig. S2A). The *GUS* construct driven by the *miR390a* promoter was introduced into poplar plants, and histological staining indicated that *miR390* was expressed weakly in the main roots but strongly in the LRs (Supplemental Fig. S2B). A genomic survey

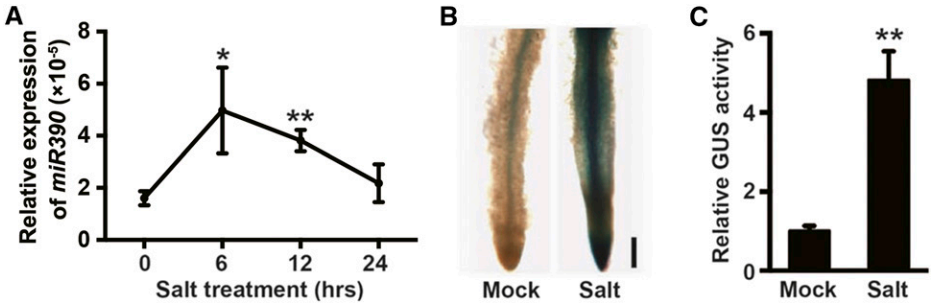

Figure 1. Salt-induced expression of *miR390* in poplar LRs. A, Time-course assay of mature *miR390* expression under salt stress. Four-week-old wild-type seedlings grown on Woody Plant Medium (WPM) were subjected to 200 mM NaCl for 0, 6, 12, and 24 h, and total roots were collected for RNA extraction. The *miR390* expression level was determined by stem-loop RT-qPCR. The *U6 snRNA* was used as a reference to normalize the expression data of *miR390*. Asterisks indicate significant differences with respect to the value for 0 h (one-way ANOVA followed by Dunnett's test for pairwise comparisons: *, $P < 0.05$ and **, $P < 0.01$; $n = 3$). B, Histological staining of the LR tip of transgenic poplar harboring the *GUS* reporter gene driven by the promoter of *miR390a* under salt treatment. Four-week-old wild-type seedlings were subjected to 200 mM NaCl for 6 h for GUS staining. Bar = 500 μm. C, Quantitative measurement of salt-induced GUS activity driven by the *miR390a* promoter in the reporter line. Salt treatment was performed as indicated in B. The values under mock treatment were normalized to 1. Error bars represent SD. Asterisks indicate significant differences with respect to the control (Student's *t* test: **, $P < 0.01$; $n = 4$).

indicated a series of stress-associated cis-elements in the promoter region of each *miR390* member (Supplemental Fig. S2C) and that *miR390* is thus possibly involved in stress-response processes. Stem-loop RT-qPCR assays revealed that *miR390* expression is induced by salt stress (Fig. 1A). Salt-induced *miR390* expression patterns in different tissues were determined by histologically staining with the GUS reporter driven by the *miR390* promoter (Fig. 1, B and C; Supplemental Fig. S2). No induced *miR390* expression was detected in the leaves (Supplemental Fig. S2, D and E). Salt-responsive GUS activity driven by the *miR390* promoter was not present in main root tips (Supplemental Fig. S2, F, G, and I), whereas *miR390* was induced weakly by salt in the stele tissues of the main roots, although induction was not statistically significant (Supplemental Fig. S2, F, H, and I). In contrast, salt strongly stimulated *PromiR390a* activity in the LR tips (Fig. 1B). GUS fluorometric measurements showed that salt stress increased *PromiR390a* activity by 5-fold in LRs containing the *PromiR390a*:*GUS* construct (Fig. 1C). *miR390* expression also was induced in LR primordia (Supplemental Fig. S2J). We conclude that salinity induces *miR390* expression in poplar plants during LR formation.

miR390 Promotes LR and Shoot Growth in Poplar

To determine whether *miR390* regulates root growth in poplar, overexpressing (OE) and short tandem target mimic (STTM)-based knockdown transgenic *miR390* poplar were generated to allow functional identification (Supplemental Fig. S3, A–C). LR development was significantly different in wild-type and transgenic 4-week-old seedlings cultivated in medium (Fig. 2A). LR length and density were significantly higher in the *miR390*-OE seedlings than in the wild-type seedlings but lower in the *miR390*-STTM lines ($P < 0.01$ and $P < 0.001$; Fig. 2, B and C). The lengths and numbers of main roots in 4-week-old *miR390* transgenic plants cultivated on medium were not affected (Supplemental Fig. S3, D and E). For 10-week-old plants cultivated in soil, the *miR390*-OE transgenic plants were larger than the wild-type plants (Fig. 2D). In contrast, *miR390* knockdown repressed shoot and root growth in the *miR390*-STTM lines (Fig. 2D). Shoot and root biomasses were 36.3% and 16.1% higher, respectively, in the *miR390*-OE lines than in the wild-type plants and 36.1% and 52.9% lower, respectively, in the *miR390*-STTM lines than in the wild-type plants (Fig. 2, E and F). We conclude that *miR390* positively regulates root (especially LR) growth and shoot growth in poplar plants.

miR390 Alleviates the Inhibition of LR Growth and Biomass Accumulation Caused by Salt Stress

It was shown previously that *miR390* regulates LR growth in Arabidopsis (Marin et al., 2010; Yoon et al., 2010). Our results indicate that salt induces *miR390* expression during LR formation in poplar plants (Fig. 1, B and C; Supplemental Fig. S2D). Therefore, we wondered whether *miR390* is involved in regulating LR development during salinity responses and the development of salt tolerance. Cutting-propagated wild-type, *miR390*-OE, and *miR390*-STTM seedlings were exposed to NaCl at concentrations of 0, 25, 50, and 75 mM for 4 weeks. LR growth was retarded in every seedling, but the wild-type and transgenic lines had different sensitivities to salt at high salt concentrations (Fig. 3A). LR length and density were inhibited slightly by 25 mM NaCl in all lines (Fig. 3, B and C; Supplemental Fig. S3F and G). The LR length and density were markedly better maintained in *miR390*-OE seedlings than in wild-type seedlings exposed to 50 and 75 mM NaCl, but 50 mM NaCl caused almost

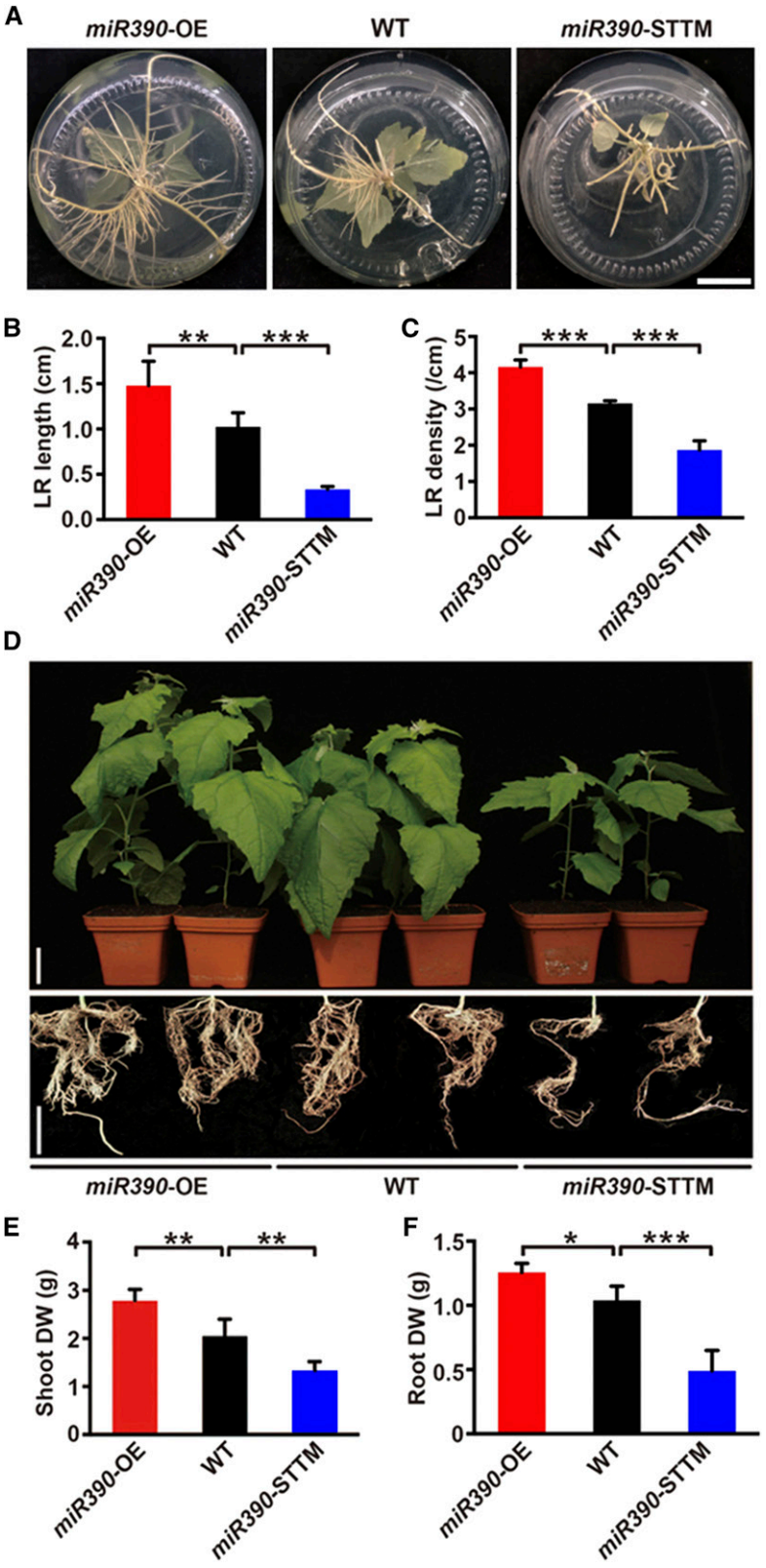

Figure 2. *miR390* positively regulates LR growth and biomass accumulation in poplar. A, LR phenotypes of seedlings of wild-type (WT), *miR390*-OE, and *miR390*-STTM lines. Cutting-propagated seedlings were cultivated in vitro for 4 weeks. Bar = 2 cm. B and C, Quantification of average LR length (B) and LR density (C) of the seedlings of wild-type, *miR390*-OE, and *miR390*-STTM lines cultivated in vitro for 4 weeks. D, Shoot and root phenotypes of wild-type, *miR390*-OE, and *miR390*-STTM plants cultivated in soil for 10 weeks. Bars = 5 cm. E and F, Quantitative measurements of shoot (E) and root (F) biomass (dry weight [DW]) of wild-type, *miR390*-OE, and *miR390*-STTM plants cultivated in soil for 10 weeks. For B, C, E, and F, error bars represent SD, and asterisks indicate statistically significant differences in one-way ANOVA followed by Dunnett's test for pairwise comparisons between wild-type and transgenic lines (*, $P < 0.05$; **, $P < 0.01$; and ***, $P < 0.001$; $n = 5$).

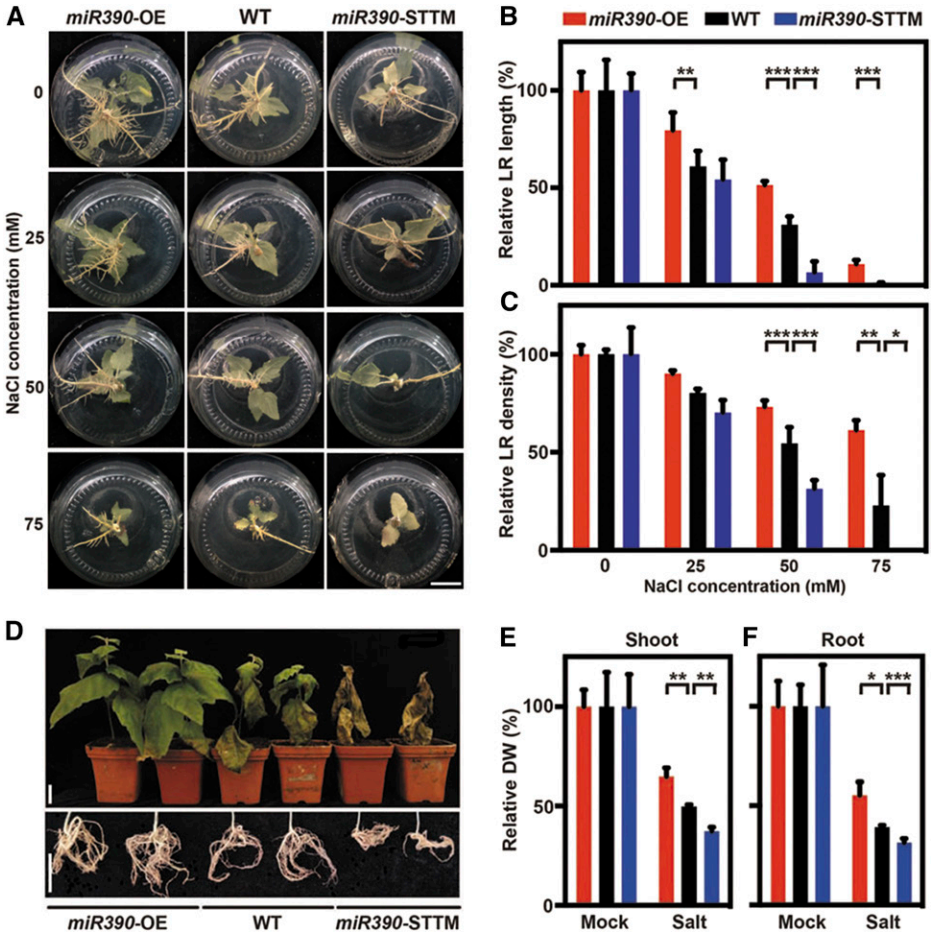

Figure 3. *miR390* enhances the salt tolerance of LR growth and biomass accumulation in poplar. A, LR phenotypes of seedlings of wild-type (WT), *miR390*-OE, and *miR390*-STTM lines under salt treatment. Cutting-propagated seedlings were cultivated in vitro and subjected to 0, 25, 50, and 75 mM NaCl for 4 weeks. Bar = 2 cm. B and C, Relative quantification of total LR length (B) and LR density (C) in seedlings of wild-type, *miR390*-OE, and *miR390*-STTM lines under salt treatment. Cutting-propagated seedlings were cultivated in vitro and subjected to 0, 25, 50, and 75 mM NaCl for 4 weeks. The values for each genotype without NaCl treatment were normalized to 100%. Nonnormalized values are given in Supplemental Figure S3, F and G. D, Shoot and root phenotypes of 10-week-old wild-type, *miR390*-OE, and *miR390*-STTM plants under salt treatment. Poplar plants were cultivated in soil for 4 weeks and watered subsequently with 200 mM NaCl for 6 weeks. Bars = 5 cm. E and F, Relative quantification of shoot (E) and root (F) biomass (dry weight [DW]) of wild-type, *miR390*-OE, and *miR390*-STTM plants under salt treatment. Poplar plants were cultivated and salinity treated as described in D. The values for each genotype under mock treatment were normalized to 100%. Nonnormalized values are given in Supplemental Figure S3, H and I. For B, C, E, and F, error bars represent SD, and asterisks indicate statistically significant differences in two-way ANOVA followed by Dunnett's test for pairwise comparisons between wild-type and transgenic lines (*, $P < 0.05$; **, $P < 0.01$; and ***, $P < 0.001$; $n = 5$).

complete suppression of LR formation in the *miR390*-STTM seedlings (Fig. 3, A–C). The function of *miR390* in response to salt stress was investigated further by irrigating 4-week-old wild-type and transgenic plants cultivated in soil with 200 mM NaCl every 2 d (Fig. 3D). This treatment caused all *miR390*-STTM plants to die within 6 weeks, but the *miR390*-OE seedlings grew well (Fig. 3D). While the wild-type plants survived, the older leaves started to wilt by this stage, indicating the effects of severe salt toxicity (Fig. 3D). Biomass accumulation in wild-type and transgenic plants exposed to salt was significantly different ($P < 0.05$, $P < 0.01$, and $P < 0.001$; Fig. 3, D–F; Supplemental Fig. S3H and I). Noticeably, shoot and root biomass was reduced by salt treatment to a greater extent in wild-type and STTM lines than in OE lines (Fig. 3, E and F). These results indicate that constitutive *miR390* expression can increase salt tolerance in poplar plants.

Targets of *tasiARFs* Are Involved in LR Development

It is well known that *miR390* directs noncoding *TAS3* transcript cleavage, generating *trans-acting small interfeing RNAs*, which posttranscriptionally target *ARF2*, *ARF3*, and *ARF4*, and therefore are called *tasiARF*s (Allen et al., 2005; Axtell et al., 2006). This action mode

is evolutionarily conserved in land plants including *Populus* spp. (Xia et al., 2017). The poplar genome has four *TAS3* loci, and the *TAS3* transcript has two *miR390* target sites (Supplemental Fig. S4A), consistent with the two-hits model (Xia et al., 2017). *TAS3.1* and *TAS3.2* can generate *tasiARFs* at two neighboring sites, and the other poplar *TAS3* members each contain a single centrally located *tasiARF* production site (Supplemental Fig. S4A). The poplar *tasiARFs* derived from *TAS3* share high similarity in sequence (Supplemental Fig. S4B). As predicted by Xia et al. (2017), *ARF3* (*ARF3.1*, *ARF3.2*, and *ARF3.3*) and *ARF4* in poplar contain dual *tasiARF*-binding sites, whereas the *ARF2* genes (*ARF2.1* and *ARF2.2*) each contains a single *tasiARF* target site (Supplemental Fig. S5). *ARF3.3* (Potri.011G059100.1) had truncated open reading frame sequences, so it was omitted from subsequent analyses.

The *miR390*-mediated molecular context in poplar was studied by testing for expression of the downstream components in transgenic *miR390*-OE plants. The *TAS3.1/3.2* transcript abundance was decreased significantly by *miR390* overexpression but increased by *miR390* knockdown ($P < 0.05$ and $P < 0.01$; Fig. 4A). Therefore, the *tasiARFs* derived from the *TAS3* transcripts preferentially accumulated in the *miR390*-OE lines but not in the *miR390*-STTM lines (Fig. 4B), indicating that *tasiARF* production in poplar is positively regulated by *miR390*. The positive regulation of *tasiARF1*, *tasiARF2*, and *tasiARF3* by *miR390* also was detected using specific oligonucleotide primers to quantify the expression of these *tasiARF* members (Supplemental Fig. S6A). RT-qPCR showed that *ARF3.1*, *ARF3.2*, and *ARF4* transcription was suppressed in the *miR390*-OE lines but enhanced in the *miR390*-STTM lines (Fig. 4C). In contrast, *ARF2* member transcription was not affected by *miR390* (Supplemental Fig. S6B). *ARF3.1*, *ARF3.2*, and *ARF4* expression was suppressed to a significant degree when plants were exposed to salt for 6 h (Fig. 4D), unlike the salt-induced accumulation of *miR390* (Fig. 1).

The transcript levels of the *tasiARF* targets *ARF3.1*, *ARF3.2*, and *ARF4* in poplar tissues were determined. *ARF4* was expressed more than the two *ARF3* homologs in all the tissues analyzed, except for old leaves (Supplemental Fig. S7). The differences were most noticeable in the roots, in which *ARF4* was expressed 14 times more than *ARF3.2* and *ARF3.1* expression was not detected (Supplemental Fig. S7). Further analyses were focused on *ARF4* because it was expressed most strongly in the root tissues. Functional complementation was performed using poplar plants to determine whether *ARF4* functions downstream in the *miR390/TAS3* context (Fig. 4, E–G). A *tasiARF*-resistant *ARF4* (*ARF4m*) containing mutated dual *tasiARF*-binding sites was introduced into the *miR390*-OE background (Supplemental Fig. S8A). *ARF4* was transcribed markedly more in the *35S:ARF4m/miR390*-OE plants than in the *miR390*-OE plants (Supplemental Fig. S8B). Phenotypic analysis indicated that introducing *ARF4m* compromised LR development of the *miR390*-OE plants (Fig. 4E), as indicated by LR length and density decreases of 52% and 35%, respectively (Fig. 4, F and G). *ARF4m* could phenotypically mimic *miR390* knockdown, as indicated by the similar phenotypes of the *ARF4m*-OE and *miR390*-STTM lines (Fig. 4, E–G). We conclude that *ARF4* can mediate *miR390*-dependent LR development.

ARF4 Negatively Regulates Plant Growth and Salt Tolerance

The vectors harboring *35S:ARF4* with the disrupted dual *tasiARF*-binding sites (*ARF4m*-OE) and RNA-interfering (RNAi)-based *ARF4* knockdown (*ARF4*-RNAi) were transformed into wild-type poplar plants to evaluate the roles of *ARF4* in the developmental phenotypes and salt responses in poplar. *ARF4m* expression in transgenic plants was determined by RT-qPCR (Supplemental Fig. S9, A and B). The transgenic plants were vegetatively propagated, and lines displaying stable phenotypes in vitro (Supplemental Fig. S9C) and in a greenhouse (Fig. 5A) were selected for further analysis. Under in vitro conditions, LR elongation and density were suppressed markedly by overexpression of the *tasiARF*-resistant *ARF4* (Supplemental Fig. S9, C–E). The dry shoot biomass was 31.9% lower in the *ARF4m*-OE plants cultivated in soil than in the wild-type plants and up to 40.7% higher in the *ARF4*-RNAi plants than in the wild-type plants (Fig. 5B). LR growth also was inhibited markedly in the *ARF4m*-OE lines but enhanced in the *ARF4*-RNAi lines (Fig. 5, A and B).

Given that *ARF4* expression was suppressed in the presence of salt (Fig. 4D), we explored whether *ARF4* contributed to salt tolerance (Fig. 5, C and D; Supplemental Figs. S9 and S10). Wild-type, *ARF4m*-OE, and *ARF4*-RNAi seedlings were exposed to NaCl at different concentrations (Supplemental Fig. S9F). After 4 weeks, LR growth was clearly inhibited in all the seedlings exposed to 50 and 75 mM NaCl. The LRs were shorter and there were fewer LRs in the *ARF4m*-OE than in the wild-type plants (Supplemental Figs. S9, F–H, and S10, A and B). In contrast, markedly less LR growth inhibition by NaCl was found in the *ARF4*-RNAi plants (Supplemental Fig. S9, F–H). Wild-type and transgenic plants were cultivated in soil and treated with 200 mM NaCl for 6 weeks. The *ARF4*-RNAi plants were larger and had more salt-tolerant phenotypes than the wild-type plants, but constitutive *tasiARF*-resistant *ARF4* expression led to retarded growth and more severe symptoms of salt toxicity (Fig. 5, C and D; Supplemental Fig. S10, C and D). We conclude that *ARF4* negatively regulates biomass accumulation and salt tolerance in poplar, in agreement with the negative regulation of *ARF4* expression by *miR390*.

Antagonistic Regulation of Auxin Signaling in LRs by *miR390* and *ARF4*

The molecular components involved in the auxin pathway were determined by RT-qPCR to determine

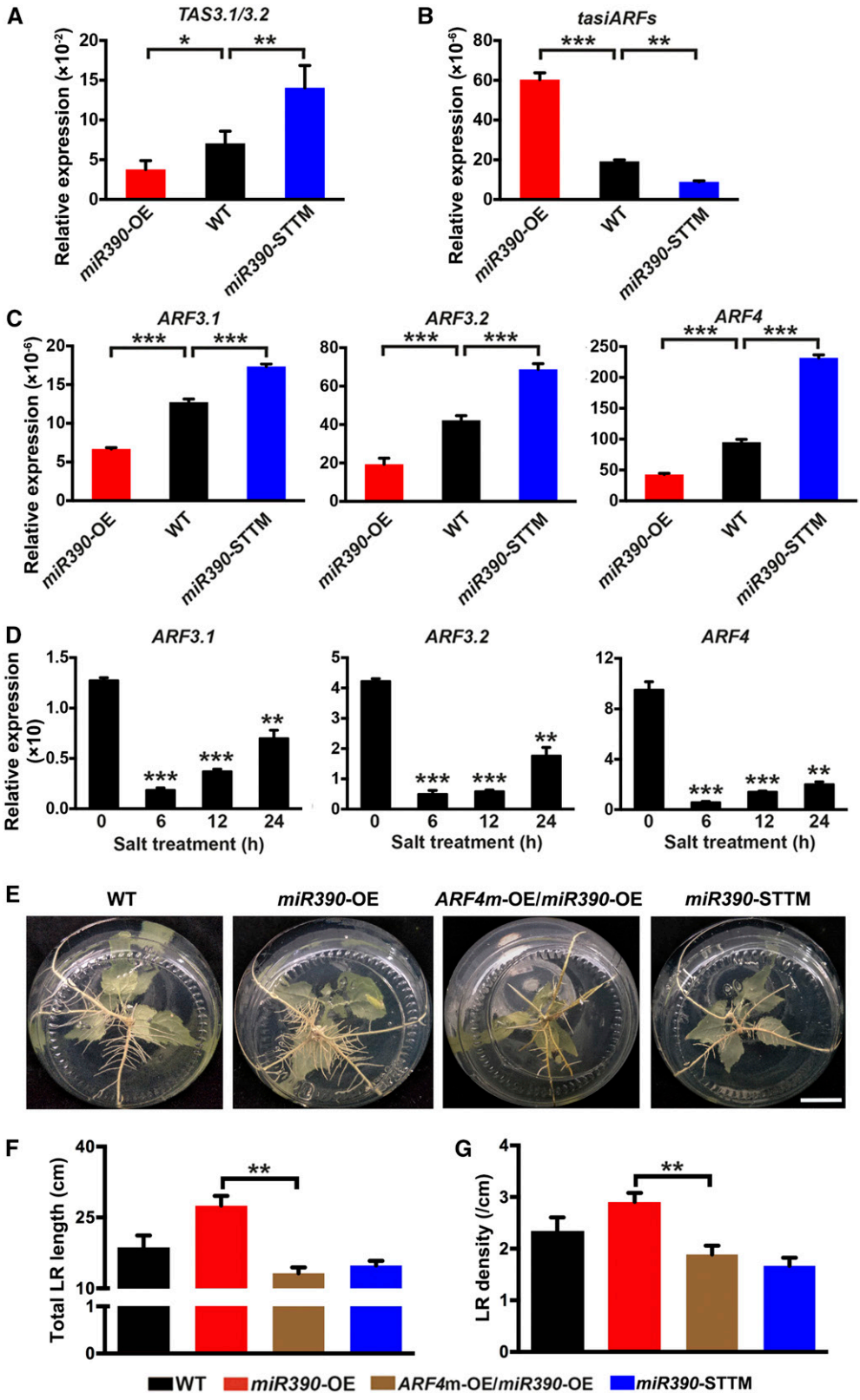

Figure 4. The *tasiARF* targets are involved in LR development. A to C, The expression levels of *TAS3.1/3.2* (A), *tasiARFs* (B), and *ARF3.1/3.2/4* (C) were quantitatively detected in wild-type (WT), *miR390*-OE, and *miR390*-STTM lines. LRs of 4-week-old seedlings cultivated in vitro were collected for RNA extraction. The expression levels of *tasiARFs* were determined by stem-loop RT-qPCR. *U6 snRNA* was used as a reference for normalizing the expression data of *miR390*. The expression levels of *TAS3*,

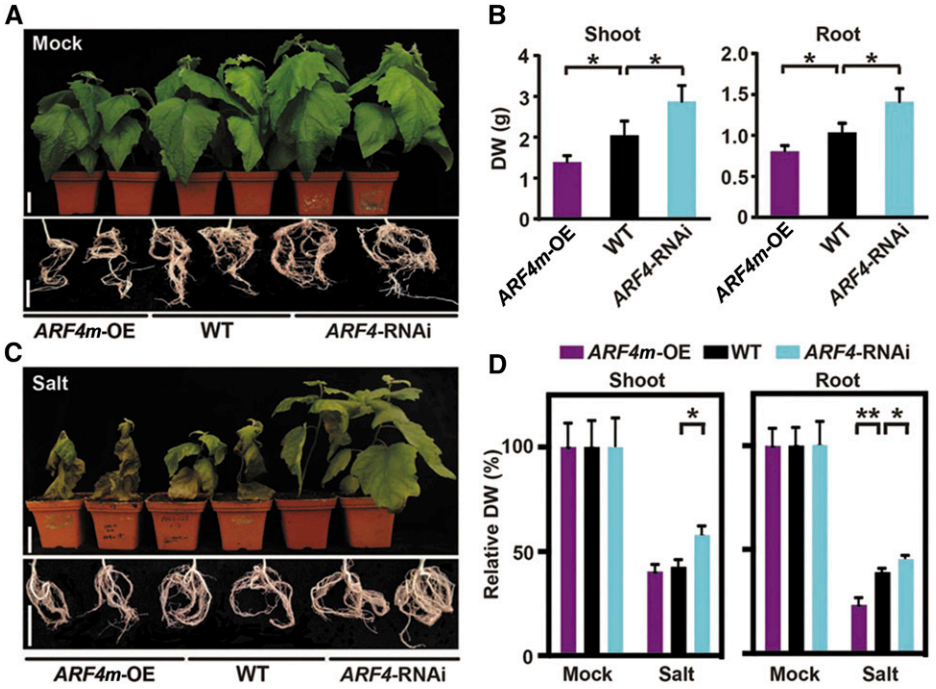

Figure 5. ARF4 negatively regulates plant growth and salt tolerance in poplar. A, Shoot and root phenotypes of wild-type (WT), *ARF4m*-OE, and *ARF4*-RNAi plants cultivated in soil for 10 weeks. Bars = 5 cm. B, Quantitative measurements of shoot and root biomass (dry weight [DW]) of wild-type, *ARF4m*-OE, and *ARF4*-RNAi plants cultivated in soil for 10 weeks. Error bars represent SD. Asterisks indicate statistically significant differences in one-way ANOVA followed by Dunnett's test for pairwise comparisons between wild-type and transgenic lines (*, $P < 0.05$; $n = 5$). C, Shoot and root phenotypes of wild-type, *ARF4m*-OE, and *ARF4*-RNAi plants under salt treatment. Poplar plants were cultivated in soil for 4 weeks and subsequently watered with 200 mM NaCl for 6 weeks. Bars = 5 cm. D, Relative quantification of shoot (E) and root (F) biomass (dry weight) of wild-type, *ARF4m*-OE, and *ARF4*-RNAi plants under salt treatment. Poplar plants were cultivated and salinity treated as described in C. The values for each genotype under mock treatment were normalized to 100%. Nonnormalized values are given in Supplemental Figure S10, C and D. Error bars represent SD. Asterisks indicate statistically significant differences in two-way ANOVA followed by Dunnett's test for pairwise comparisons between wild-type and transgenic lines (*, $P < 0.05$ and **, $P < 0.01$; $n = 5$).

the effect of *miR390/TAS3/ARF* on auxin accumulation and the auxin response. A few typical *Aux/IAA* (*IAA3.1* and *IAA3.2*) and *GH3* (*GRETCHEN HAGEN3*; *GH3.2* and *GH3.5*) genes (which belong to classic categories of early auxin-responsive genes in various plant species; Guilfoyle, 1999) were transcribed more in the *miR390*-OE and *ARF4*-RNAi lines and less in the *miR390*-STTM and *ARF4m*-OE lines (Fig. 6A). Similar expression patterns were found in these transgenic lines for several *PIN* genes (Fig. 6B), which are involved in polar auxin transport in *Populus* spp. root tissues (Liu et al., 2014).

Local auxin accumulation is an early signal of LR formation (Dubrovsky et al., 2008); therefore, we investigated whether *miR390* and *ARF4* affect endogenous auxin signaling in the transgenic lines. The *DR5*:*GFP* reporter, a biosensor of in vivo auxin signaling

Figure 4. (*Continued.*)
ARF3.1, *ARF3.2*, and *ARF4* were determined by RT-qPCR, and *18S rRNA* was used as a reference for normalization. Error bars represent SD. Asterisks indicate statistically significant differences in one-way ANOVA followed by Dunnett's test for pairwise comparisons between wild-type and transgenic lines (*, $P < 0.05$; **, $P < 0.01$; and ***, $P < 0.001$; $n = 3$). D, Time-course assays of *ARF3.1*, *ARF3.2*, and *ARF4* expression levels to salt treatment. Four-week-old wild-type seedlings grown on WPM were subjected to 200 mM NaCl for 0, 6, 12, and 24 h, and LRs were collected for RNA extraction. The expression levels of *ARFs* were determined by RT-qPCR. *18S rRNA* was used as a reference for normalization. Error bars represent SD. Asterisks indicate significant differences with respect to the values for 0 h (one-way ANOVA followed by Dunnett's test for pairwise comparisons: **, $P < 0.01$ and ***, $P < 0.001$; $n = 3$). E, LR phenotypes of *ARF4m* transgenic seedlings in the *miR390*-OE background. Cutting-propagated seedlings of wild-type, *miR390*-OE, *ARF4m*-OE/*miR390*-OE, and *miR390*-STTM lines were cultivated on WPM for 4 weeks. Bar = 2 cm. F and G, Quantitative measurements of total LR length (F) and LR density (G) of *ARF4m* transgenic seedlings in the *miR390*-OE background. Seedlings of wild-type and transgenic lines were cultivated as described in E. Error bars represent SD. Asterisks indicate statistically significant differences in one-way ANOVA followed by Dunnett's test for pairwise comparisons between *ARF4m*-OE/*miR390*-OE and *miR390*-OE or *miR390*-STTM (**, $P < 0.01$; $n = 5$).

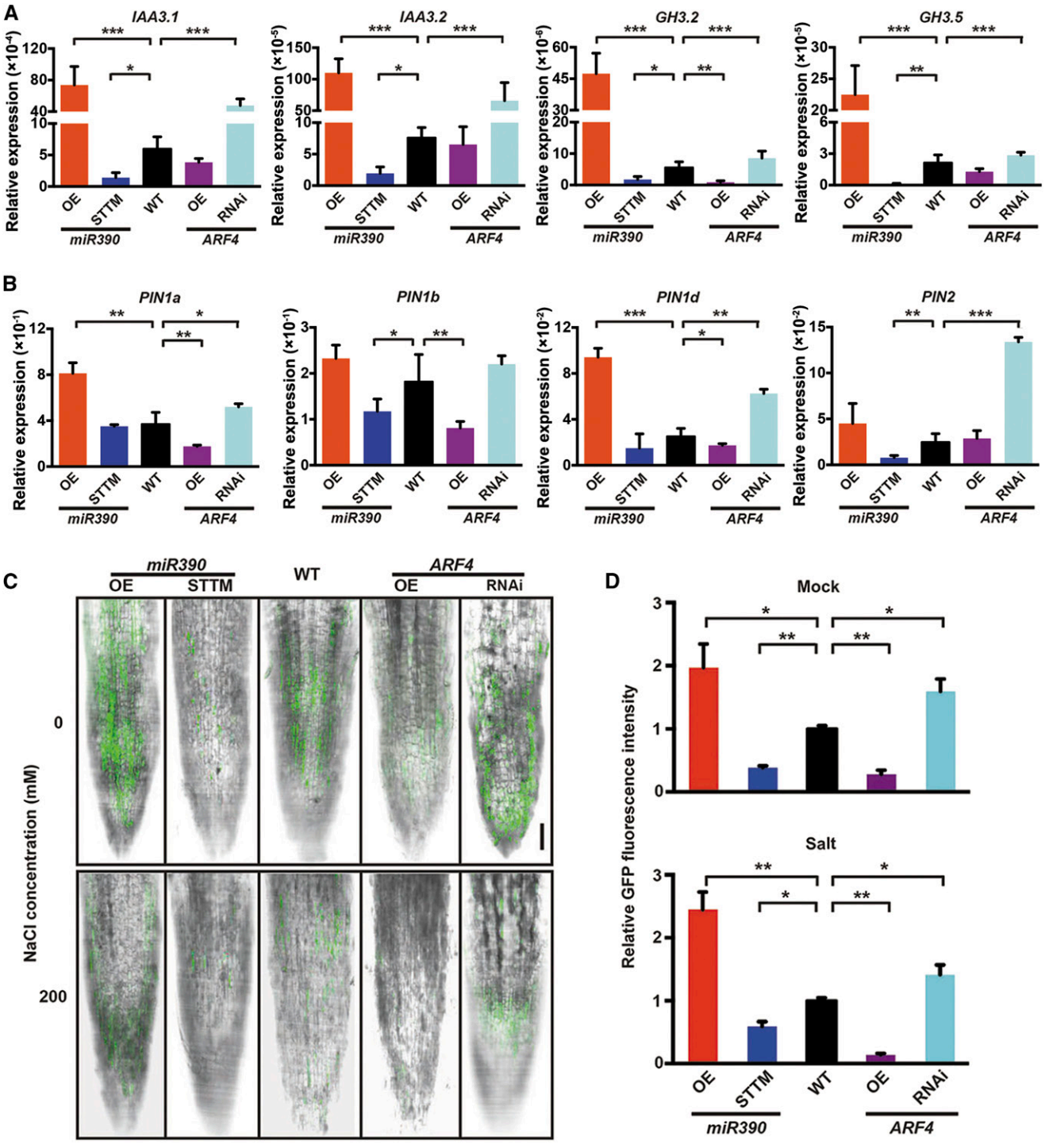

Figure 6. Auxin accumulation is altered by *miR390* and *ARF4* in LR tips. A, Expression levels of typical auxin-responsive genes, including *IAA3.1/3.2* and *GH3.2/3.5*, in LRs of *miR390*/*ARF4* transgenic lines. LRs of 4-week-old seedlings of wild-type (WT), *miR390*-OE/STTM, and *ARF4m*-OE/*ARF4*-RNAi lines cultivated in vitro were collected for RT-qPCR assay. *18S rRNA* was used as a reference for normalization. Error bars represent SD. Asterisks indicate statistically significant differences in one-way ANOVA followed by Dunnett's test for pairwise comparisons between wild-type and transgenic lines (*, $P < 0.05$; **, $P < 0.01$; and ***, $P < 0.001$; $n = 3$). B, Expression quantification of select *PIN* genes, including *PIN1a*, *PIN1b*, *PIN1d*, and *PIN2*, in root tissues of *miR390*/*ARF4* transgenic plants. RT-qPCR assay and statistical analysis were performed as described in A. C, Detection of GFP fluorescence driven by the auxin-responsive *DR5* promoter in LR tips of the *miR390*/*ARF4* transgenic lines under salt treatment. Four-week-old seedlings of wild-type, *miR390*-OE/STTM, and *ARF4m*-OE/*ARF4*-RNAi lines harboring the DR5 promoter were subjected to 0 mM (mock) or 200 mM NaCl (salt) for 24 h. LR tips were detected for GFP fluorescence via

(Ottenschläger et al., 2003), was introduced to indicate *miR390/ARF4*-induced modifications of the endogenous auxin concentration and signaling in the LR tips (Fig. 6C). The GFP fluorescent signals driven by the auxin-responsive DR5 promoter were stronger in the LR tips of the *miR390*-OE and *ARF4*-RNAi plants than in the wild-type plants but were weaker in the *miR390*-STTM and *ARF4m*-OE plants than in the wild-type plants (Fig. 6, C and D). Exposure to salt decreased *DR5*:*GFP* expression in the wild-type plants, and the effect was much stronger in the *miR390*-STTM and *ARF4m*-OE plants than in the wild-type plants (Fig. 6, C and D). Conversely, *DR5*:*GFP* expression was less affected in the salt-stressed *miR390*-OE and *ARF4*-RNAi plants than in the salt-stressed wild-type plants (Fig. 6, C and D). These results suggest that, in poplar plants, *miR390* and *ARF4* antagonistically regulate endogenous auxin signaling during LR development in response to salinity.

IAA17 Can Block *miR390/ARF4*-Mediated LR Development under Salt Stress

As reported in Arabidopsis, salt inhibition of root meristematic activity is caused by modified *PIN*-mediated auxin accumulation and *Aux/IAA*-dependent auxin signaling (Liu et al., 2015). Modulated *PIN* gene expression and auxin signaling as indicated by the DR5 sensor in the poplar LRs (Fig. 6) suggest that the auxin pathway may mediate *miR390/ARF4*-regulated LR growth and salt tolerance. Firmly establishing auxin-dependent *miR390/ARF4* regulation of salt-responsive LR growth required us to investigate what happens to the *miR390/ARF4* root phenotypes when auxin signaling is blocked. Nucleus-localized Aux/IAA proteins are key repressors of auxin signaling (Rouse et al., 1998). These proteins usually contain short amino acid sequences (VGWPPV) called Degron motifs, which allow auxin-induced protein turnover via the E3 ubiquitin ligase complex SCF^{TIR1} (Worley et al., 2000; Tan et al., 2007). Salt stress in Arabidopsis enhances the protein stabilization of IAA17, a canonical Aux/IAA protein that represses auxin signaling (Liu et al., 2015). Mutation of the Degron motif in IAA17, which compromises auxin-dependent protein instability, correspondingly leads to the root tissues becoming insensitive to salt stress (Liu et al., 2015). The poplar genome has two homologous members of *IAA17*, called *IAA17.1* and *IAA17.2* (Supplemental Fig. S11A). The protein IAA17.1 is more similar than IAA17.2 to Arabidopsis IAA17 and has an identical Degron motif in domain II to the motif in Arabidopsis IAA17 (Supplemental Fig. S11A). RT-qPCR showed that *IAA17.1* is preferentially expressed in the root tissues (Supplemental Fig. S11B). The promoter-driving GUS reporter assays confirmed that *IAA17.1* is expressed in the roots, especially in the LR primordia and tips (Supplemental Fig. S11C).

The auxin-dependent regulation of salt-induced root modifications in poplar by *miR390/ARF4* was tested using IAA17.1 to block auxin signaling. We first determined whether the stability of the poplar IAA17.1 protein was affected by auxin and salt in the same way as the Arabidopsis IAA17 protein (Fig. 7A). Evolutionary conservation of auxin signaling, including the Aux/IAA protein family (Paponov et al., 2009), means that transient expression in a heterologous system can be used as an efficient method of studying the stability of Aux/IAA proteins in response to auxin (von Behrens et al., 2011; Ludwig et al., 2014). Therefore, auxin/salt-responsive IAA17.1 protein turnover was monitored by fusing the protein with a GFP tag in a transiently expressed *Nicotiana benthamiana* leaf epidermis. As expected, auxin induced IAA17.1 protein instability, as indicated by decreased GFP fluorescence in leaf epidermal cells exposed to indole-3-acetic acid (Fig. 7A). In contrast, the number of green fluorescent cells and GFP fluorescence increased in the presence of NaCl, indicating that IAA17.1 protein turnover was suppressed (Fig. 7A). To determine whether the Degron motif mediates the change in protein turnover caused by auxin and salt, a Degron-mutated IAA17.1 protein, IAA7.1m, with the first Pro replaced through Ser substitution (Supplemental Fig. S11D), was generated as described previously (Li et al., 2011). GFP fluorescence was stronger in leaf epidermal cells transiently transformed by IAA17.1m with an impaired Degron motif than in the cells transformed by the wild-type IAA17.1 form (Fig. 7A). The fluorescence emitted by IAA17.1m-GFP was affected neither by exogenous auxin nor by the presence of salt (Fig. 7A), indicating that the auxin-responsive IAA17.1 protein was stabilized by salt, depending on the Degron motif. Therefore, the auxin/salt-resistant version of IAA17.1 (IAA17.1m) was introduced into the *miR390*-OE and *ARF4*-RNAi lines (Supplemental Fig. S11, E and F) to allow the auxin-dependent machinery of *miR390/ARF4*-mediated salt tolerance of LR growth to be studied. Transgenic *IAA17.1m*-OE/*miR390*-OE and *IAA17.1m*-OE/*ARF4*-RNAi plants were more sensitive to salt stress than *miR390*-OE and *ARF4*-RNAi plants in terms of LR inhibition (Fig. 7B). The LR lengths and densities in the *miR390*-OE/*ARF4*-RNAi plants were at least partly recovered, compared with those in the wild type, by introducing IAA17.1m in the presence of salt (Fig. 7, C and D). These results

Figure 6. (*Continued.*)
confocal microscopy. Bar = 10 μm. D, Quantitative measurement of GFP fluorescent signals driven by the auxin-responsive *DR5* promoter in LR tips of the *miR390/ARF4* transgenic lines under salt treatment. Salt treatment and fluorescence detection were conducted as described in C. Fluorescence was quantified via the software FV10 ASW (Olympus). Error bars represent SD. Asterisks indicate statistically significant differences in one-way ANOVA followed by Dunnett's test for pairwise comparisons between wild-type and transgenic lines (*, $P < 0.05$ and **, $P < 0.01$; $n = 5$).

indicate that *miR390/TAS3/ARF*-dependent regulation of salt-responsive LR development in poplar plants is mediated by auxin signaling.

DISCUSSION

Salt stress profoundly affects the architecture of plant roots. Affected plants show symptoms of toxicity, and their root systems display active salt-responsive developmental plasticity (e.g. growth maintenance and halotropism), which strongly facilitates increased salt tolerance (Galvan-Ampudia and Testerink, 2011; Galvan-Ampudia et al., 2013). We found that *miR390*, an evolutionarily conserved miRNA in plants, is induced by salt during the formation of LR in poplar plants. Phenotypic analysis and functional complementation via stable transformations in poplar suggested that *miR390/TAS3/ARF4*-dependent salt tolerance occurs via the maintenance of auxin-mediated LR growth. Our results provide evidence that salt-inducible *miR390* expression is an adaptive strategy for maintaining growth in poplar plants in saline environments.

In in vitro tests, the root systems of 4-week-old poplar seedlings usually have two types of roots: several stem-borne main roots and many LRs emerging from the main roots. The lengths and densities of LRs were both found to be positively regulated by *miR390* (Fig. 2, B and C), whereas the lengths and numbers of main roots were not affected (Supplemental Fig. S3, D and E). These results show that *miR390* specifically regulates LR phenotypes, probably through expression to different degrees in main roots and LRs (Supplemental Fig. S2B). This accords with the *miR390/TAS3/ARF*-dependent LR formation in Arabidopsis described previously (Marin et al., 2010; Yoon et al., 2010). Salt-induced *miR390* expression also was specific to LR development. Salt-inducible *miR390* expression was found in both LR meristems and LR primordia (Fig. 1B; Supplemental Fig. S2D) and accounts for the maintenance of both LR elongation and initiation. Weak induction in stele tissues of main roots was found, but no salt-stimulated *miR390* expression occurred in the main root tips (Supplemental Fig. S2D). The variable salt-inducible expression patterns matched the *miR390*-dependent LR-specific poplar phenotypes. These results suggest that root type-specific mechanisms responsive to salt occur in poplar plants, as proposed for Arabidopsis (Geng et al., 2013).

Auxin is the main triggering signal for root development and plays key roles in salt-induced root morphological and meristematic modulations (Galvan-Ampudia and Testerink, 2011; Liu et al., 2015). The current auxin signaling model suggests that auxin is transduced into nuclei to drive auxin-responsive gene expression (Vanneste and Friml, 2009). *IAA3* is a typical early auxin-responsive gene that can affect the sensitivity of LR formation in poplar to auxin (Nilsson et al., 2008). *GH3.2* and *GH3.5* belong to the primary auxin-responsive *GH3* gene family that encodes IAA-amide synthetases, mutations of which increase the resistance of LR formation to exogenous auxin (Staswick et al., 2005). Modulated expression of these primary auxin-responsive genes (Fig. 6A) shows the *miR390/ARF4*-regulated auxin responses. The distribution of auxin is determined mainly by PIN-mediated auxin transport in poplar plants (Palme and Gälweiler, 1999; Friml et al., 2002). In Arabidopsis, PIN1 displays salt-inhibited protein accumulation in the root meristem (Liu et al., 2015) and PIN2 mediates salt-induced halotropism in the root system (Galvan-Ampudia et al., 2013). The PIN1 and PIN2 members are expressed similarly in different poplar root tissues, including LR tips (Liu et al., 2014). The transcript abundances of several *PIN1/PIN2* genes (Fig. 6C) implied that *miR390/ARF4*-dependent local accumulation of auxin could occur. The subsequent DR5-indicated auxin signaling reveals that *miR390/ARF4* orchestrates the accumulation of auxin in LRs under normal and saline conditions (Fig. 6). More importantly, switching off auxin signaling by stably expressing an auxin/salt-resistant version of the IAA17 protein decreased salt-responsive LR growth regulated by *miR390/ARF4* to a remarkable degree (Fig. 7). These results together demonstrate that the *miR390/ARF4* module maintains salt-tolerant LR growth by attenuating the inhibition of auxin signaling by salt stimuli.

In addition to maintaining LRs in a saline environment, *miR390* alleviates salt toxicity to aboveground growing tissues (Fig. 3, D and E). No salt-inducible expression was detected in the leaves (Supplemental Fig. S2D), so the modulation of downstream molecular events mediated by *miR390* may not occur in polar shoot tissues. It has been suggested that larger plants are more salt tolerant than smaller plants (Julkowska et al., 2016). Therefore, we speculate that salt-tolerant phenotypes of aboveground growth in *miR390*-OE lines may be a secondary effect of maintaining root development. Ion exclusion and osmotic tolerance may play roles in these effects (Roy et al., 2014); therefore, further evidence is required to account for salt resistance caused by *miR390*.

The results of this study allowed a model of *miR390/ARF4*-dependent LR growth in poplar under normal and saline conditions to be devised (Fig. 8). *miR390* produces *TAS3*-derived *tasiARFs* that target *ARF4* transcripts (Figs. 4 and 8A). The repression of *ARF4* releases auxin, which triggers LR initiation and elongation in poplar plants (Figs. 6 and 8A). In highly saline environments, salt markedly inhibits auxin signaling and induces *miR390* expression (Figs. 6 and 8B, left). The salt-induced expression of *miR390* stimulates the production of *tasiARFs* for the degradation of *ARF4* transcripts (Figs. 1, 4, and 8, left). Attenuated expression of *ARF4* facilitates the maintenance of auxin signaling against salt inhibition (Figs. 5, 6, and 8B, left). If the salt induction of *miR390* did not occur, auxin signaling and LR formation would be more seriously inhibited by salt (Fig. 8B, right). The *miR390/tasiARF/ARF4* module is thereby essential for sustaining LR formation under salinity and salt-tolerant plant growth. In summary, the

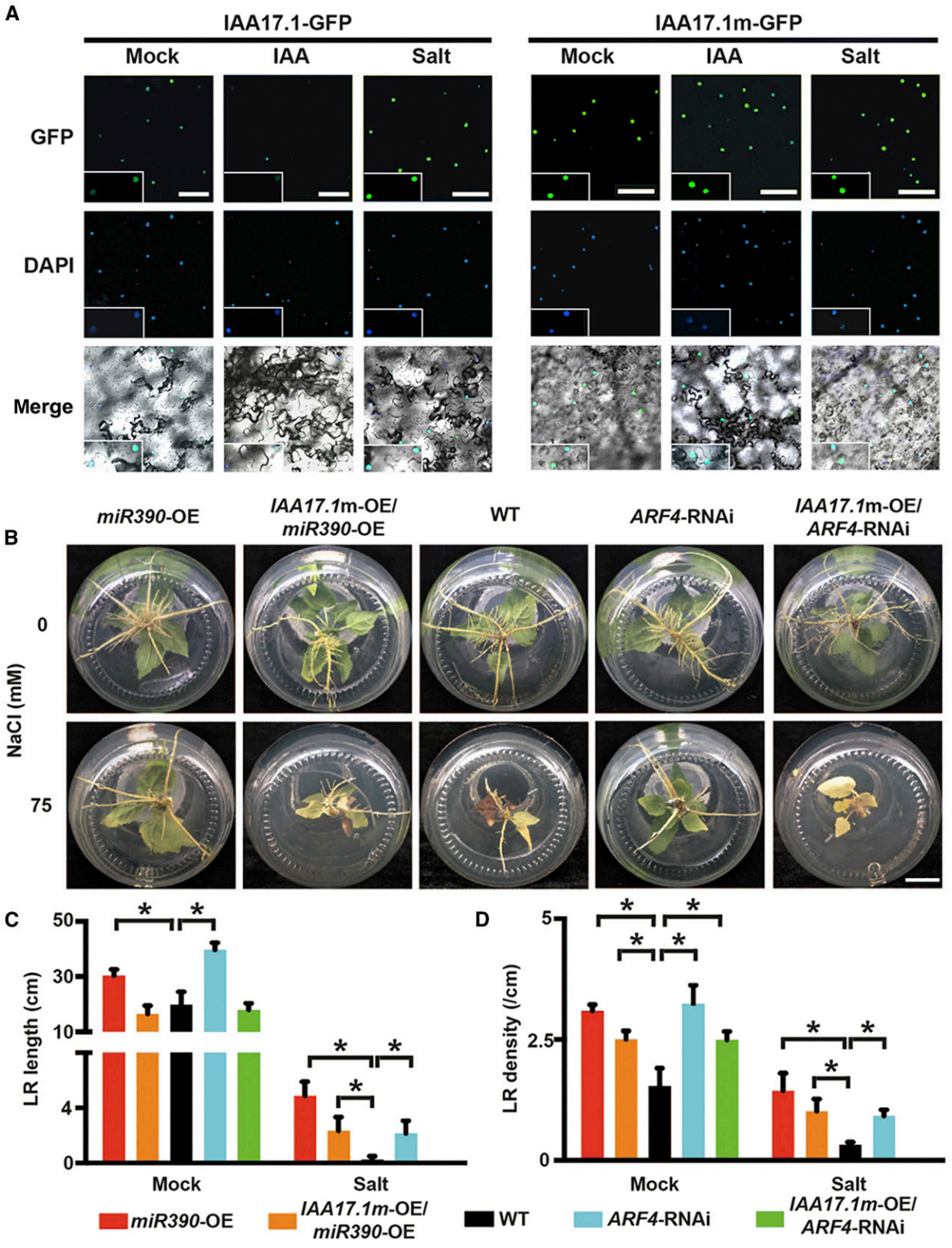

Figure 7. IAA17.1, an Aux/IAA protein, is required for *miR390/ARF4*-mediated LR development under salt stress. A, Auxin/salt-responsive protein stability of IAA17.1 indicated by fused GFP tag. IAA17.1m, an auxin-resistant form of IAA17.1, was generated by a Ser substitution for the first Pro in the Degron motif of domain II (Supplemental Fig. S11D). GFP-tagged IAA17.1 and IAA17.1m were transiently expressed in epidermal cells of *N. benthamiana* leaves via *Agrobacterium tumefaciens*-mediated

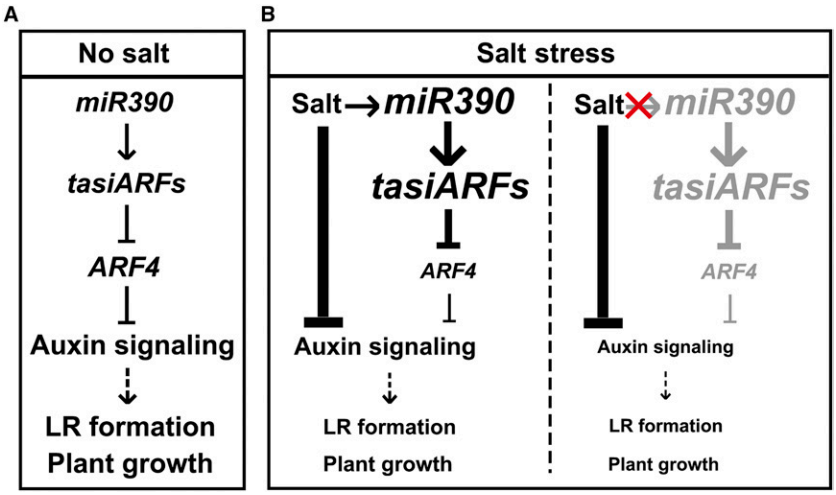

Figure 8. Proposed model for *miR390/ARF4*-dependent poplar LR growth under normal and salt conditions. A, *miR390* produces *TAS3*-derived *tasiARFs* that target *ARF4* transcripts via direct binding. The repression of *ARF4* releases auxin signaling for LR initiation and elongation. B, Left, Salt remarkably inhibits auxin signaling and induces *miR390* expression. The salt-induced expression of *miR390* stimulates the production of *tasiARFs* for the degradation of *ARF4* transcripts. Attenuated expression of *ARF4* facilitates the maintenance of auxin signaling against salt inhibition. Right, If the salt induction of *miR390* does not occur, auxin signaling and LR formation are more seriously inhibited by salt. The *miR390/tasiARF/ARF4* module is thereby essential for sustaining LR formation under salinity and salt-tolerant plant growth. Arrows represent a positive regulatory action of one component on another. Lines ending with a trait represents a negative regulatory action. The font size of words and the thickness of arrows/lines in B indicate positive (larger/thicker) or negative (smaller/thinner) regulation compared with that under the normal condition (no salt). The red cross and gray words (right) indicate the hypothetical absence of salt induction of the *miR390/tasiARFs/ARF4* module.

miR390/TAS3/ARF4 module is involved in LR maintenance against salt toxicity by modulating auxin signaling. This is a molecular strategy for improving the adaptability of poplar plants to saline conditions.

MATERIALS AND METHODS

Gene Cloning and Vector Construction

The precursor of *miR390a* was amplified using the primers *Pre-miR390a*-OE-fw/rv (Supplemental Table S1) from genomic DNA of *Populus trichocarpa* and ligated via TA-cloning into the pCXSN vector (Chen et al., 2009) under the control of the cauliflower mosaic virus *35S* promoter. The STTM-based knockdown construct of *miR390* was generated according to a previous report (Yan et al., 2012). Briefly, a pair of primers mimicking the sequences of the *miR390*-binding site with an insertion of AGA (*miR390*-STTM-*Bam*HI-fw/rv; Supplemental Table S1) was used for the amplification of the 88-bp spacer (Supplemental Fig. S3B) from a de novo synthesized oligonucleotide fragment containing the spacer sequence. The PCR product was then constructed into the pCXSN vector via *Bam*HI restriction sites (Supplemental Fig. S3B). A promoter fragment of 1,509 bp upstream of the *miR390* precursor was amplified from the genomic DNA of *Populus tomentosa* using the primers *Pro-miR390-Bam*HI-fw/rv (Supplemental Table S1) and constructed via *Bam*HI restriction sites into pXGUS-P to drive the expression of *GUS* (Chen et al., 2009). The full-length coding sequence of *ARF4* was amplified from the cDNA of *P. trichocarpa* using the primers *ARF4*-CDS-fw/rv (Supplemental Table S1) and constructed into pCXSN for sequencing via homologous recombination. Due to the presence of dual *tasiARF*-binding sites, overlap PCR was conducted twice to generate *tasiARF*-resistant *ARF4* (*ARF4m*) using the primer pairs *ARF4-Bgl*II-fw/*ARF4m*-1-rv, *ARF4m*-1-fw/*ARF4-Bgl*II-rv, *ARF4-Bgl*II-fw/*ARF4m*-2-rv, and *ARF4m*-2-fw/*ARF4-Bgl*II-rv (Supplemental Table S1). The resulting *ARF4m* fragment was constructed into modified pCAMBIA1305 with the replacement of hygromycin by kanamycin for positive selection of transgenic plants via *Bgl*II restriction sites. The *ARF4*-RNAi vector was constructed via intron-containing hairpin RNA silencing (Wesley et al., 2001). Briefly, a 223-bp sequence of *ARF4* was amplified using the primer pair *ARF4*-RNAi-*Bam*HI-fw/*ARF4*-RNAi-rv (Supplemental Table S1). Meanwhile, for a spacer, a 388-bp fragment of the *GUS* gene was prepared using the primers Spacer-RNAi-fw/rv (Supplemental Table S1), both of which contain the reverse complementary

Figure 7. (*Continued.*)
infiltration. The transformed leaves were treated with auxin or salt for 2 h: 50 μM cycloheximide (CHX, an inhibitor of protein synthesis in eukaryote cells; mock treatment), 50 μM CHX and 20 μM indole-3-acetic acid (IAA; auxin treatment), and 50 μM CHX and 200 mM NaCl (salt treatment). The nuclei of transfected epidermal cells were indicated by 4,6-diamidino-2-phenylindole (DAPI; working solution, 1 μg mL^{-1}). GFP and DAPI fluorescence was determined via confocal microscopy. Bars = 25 μm. B, Root phenotypes of *IAA17.1m* transgenic seedlings in the *miR390*-OE or *ARF4*-RNAi background under mock and salt treatment. The cutting-propagated seedlings of the wild type (WT), *miR390-OE*, *IAA17.1m*-OE/*miR390*-OE, *ARF4*-RNAi, and *IAA17.1m*-OE/*ARF4*-RNAi were cultivated in vitro and subjected to 0 mM (mock) or 75 mM NaCl (salt) for 4 weeks. Bar = 2 cm. C and D, Quantification of total LR length (C) and LR density (D) of *IAA17.1m* transgenic seedlings in the *miR390*-OE or *ARF4*-RNAi background under mock and salt treatment. Salt treatment was performed as described in B. Error bars represent SD. Asterisks indicate statistically significant differences in two-way ANOVA followed by Dunnett's test for pairwise comparisons between wild-type and transgenic lines (*, $P < 0.05$; $n = 5$).

sequence of the primer *ARF4*-RNAi-rv at the 5′ end. Subsequently, the hairpin structure harboring sense/antisense arms separated by an oligonucleotide fragment of *GUS* was generated via overlap PCR using *ARF4*-RNAi-*Bam*HI-fw and cloned into pCXSN via *Bam*HI restriction sites. The full-length coding sequence of *IAA17.1* was amplified from cDNA using the primers *IAA17.1*-stop-*Bam*HI-fw/rv (Supplemental Table S1) and constructed into modified pCAMBIA1305 with the kanamycin-resistant gene under the control of the *35S* promoter. The mutation of its Degron motif (*IAA17.1m*; Supplemental Fig. S11B) was introduced via overlap PCR using the primer pairs *IAA17.1*-stop-*Bam*HI-fw/*IAA17.1m*-rv and *IAA17.1m*-fw/*IAA17.1*-stop-*Bam*HI-rv (Supplemental Table S1). The sequences of *IAA17.1* and *IAA17.1m* without the TGA stop codon were subcloned into pCAMBIA1300-GFP to fuse with the GFP tag using the primers *IAA17.1*-non-stop-*Bam*HI-fw/rv (Supplemental Table S1). A promoter region of 1,809 bp upstream of the ATG start codon of *IAA17.1* was amplified using the primers *Pro-IAA17.1-Sal*I-fw/*Pst*I-rv (Supplemental Table S1) and cloned into pXGUS-P via TA-cloning to drive *GUS* expression. Multiple sequence alignments were conducted using DNAMAN8 (Lynnon Biosoft), and phylogenetic construction was performed with MEGA6.06 (Tamura et al., 2013).

Generation of Transgenic Poplar Lines

For functional characterization, the pCXSN vectors for the overexpression of *miR390a*, *ARF4m*, and *IAA17.1m*, *miR390*-STTM and *ARF4*-RNAi, were stably transformed into *P. tomentosa* (clone 741) plants. For functional complementation, *35S*:*ARF4m* was transformed into the *miR390*-OE line while *35S*:*IAA17.1m* was transformed into the *miR390*-OE or *ARF4*-RNAi transgenic line. For promoter analyses, the pXGUS-P vectors harboring the *GUS* gene driven by the promoter of *miR390a* or *IAA17.1* were transformed into wild-type plants. For the detection of auxin signaling, the *DR5-GFP* plasmid was transformed into the wild-type, *miR390*-OE/STTM, and *ARF4m*-OE/*ARF4*-RNAi lines, respectively. Genetic transformation of poplar was conducted via *Agrobacterium tumefaciens*-mediated infiltration of leaf discs as described previously (Jia et al., 2010). PCR genotyping for positive transgenic lines was performed through amplifying hygromycin- or kanamycin-resistant genes from genomic DNA (with primers Hyg or Kana-fw/rv; Supplemental Table S1).

Growth Conditions and Salt Treatment of Poplar

Transgenic and wild-type poplar plants were propagated via in vitro microcutting. Shoot segments of 3 to 4 cm with two to three young leaves were cut from sterilized seedlings and cultivated on sterile WPM (Jia et al., 2010) for 4 weeks at 25°C with 16 h of light of 5,000 lx and 8 h of dark. For salt stress, shoot microcuttings were cultivated for 4 weeks on the WPM supplemented with 25, 50, and 75 mM NaCl in parallel with the salt-free mock treatment. A digital camera (EOS 550D; Canon) was used to take photographs of root systems, and ImageJ (https://imagej.nih.gov/ij/) was used to quantify root parameters. The experiments under in vitro conditions were conducted using three batches of plant materials including five biological replicates (an individual plant represents a biological replicate) each time.

For physiological experiments in soil, 4-week-old microcutting-propagated plants of wild-type and transgenic lines were transferred to soil in pots and cultivated for 4 weeks in a greenhouse at 23°C to 25°C with light of 10,000 lx under a 16/8-h day/night cycle. The plants were irrigated subsequently with 0 (mock treatment) or 200 mM NaCl (salt treatment) every 2 d for 6 weeks. Afterward, root and aboveground tissues were collected for dry weight measurement. The experiments in soil were performed using two batches of plant materials including five biological replicates (an individual plant represents a biological replicate) each time.

RT-qPCR

Root tissues of 4-week-old seedlings of wild-type and transgenic lines cultivated under in vitro conditions were frozen in liquid nitrogen for gene expression assays via RT-qPCR. Four-week-old wild-type seedlings were subjected to 200 mM NaCl for 6, 12, and 24 h, and their root tissues were collected in liquid nitrogen for RNA isolation. The RNAs for tissue-specific expression quantification were prepared from 10-week-old plants grown in soil, including the tissues of roots, stem, the first two leaves on the top (young leaves), the fifth and sixth leaves (middle leaves), and the two lowest leaves aboveground (old leaves). Trizol reagent was used for total RNA extraction from the tissues frozen in liquid nitrogen according to the product manual. cDNA synthesis and RT-qPCR were performed using the PrimeScript RT Reagent Kit (Takara) in a TP800 Real-Time PCR machine (Takara) as described by the instructions. The poplar *18S rRNA* was used as a reference gene for normalization of the expression data. The transcript levels of *TAS3.1/3.2*, *ARF4/3.1/3.2/2.1/2.2/2.3/2.4/2.5*, *IAA17.1/3.1/3.2*, *GH3.2/3.5*, and *PIN1a/1b/1d/2* were determined using gene-specific primer pairs (Supplemental Table S1). The expression levels of mature *miR390* and *tasiARFs* were assayed via stem-loop RT-qPCR, a method for the sensitive and specific quantification of small RNAs (Varkonyi-Gasic et al., 2007). The *U6 snRNA* was used for data normalization of *miR390* and *tasiARF* expression. The primers for stem-loop reverse transcription, the specific forward primers, and the universal reverse primer are listed in Supplemental Table S1. Due to nucleotide variations at the 3′ end of *tasiARF1*, *tasiARF2*, and *tasiARF3*, degenerate primers were designed for stem-loop reverse transcription of *tasiARFs* (Supplemental Table S1). The expression data were calculated with the ΔΔCt method. The RT-qPCR assays were performed in three biological replicates (a mixture of at least two individual plants represents a biological replicate) together with three technical replicates for each gene.

GUS Staining

The positive GUS reporter lines driven by the promoter of *miR390a* and *IAA17.1* were cultivated on WPM for 4 weeks and then histologically stained. For the detection of salt-inducible expression, the *miR390a*-promoter-GUS seedlings were subjected to 200 mM NaCl for 6 h before histological staining. The seedlings were incubated in staining buffer (0.5 M Tris, pH 7, and 10% (v/v) Triton X-100) with 1 mM 5-bromo-4-chloro-3-indolyl-D-glucuronide at 37°C for 6 h in dark. Chlorophyll was removed using an ethanol series: 20%, 35%, and 50% (v/v) ethanol at room temperature for 30 min each. The chlorophyll-free stained seedlings were observed with an Olympus SZX16 microscope and documented with a camera (Olympus DP73).

DR5-GFP Detection

The *DR5-GFP* plasmid (Ottenschläger et al., 2003) was stably transformed into the positive poplar transgenic lines of the wild type, *miR390*-OE/STTM, and *ARF4m*-OE/RNAi using *A. tumefaciens*-mediated infiltration of leaf discs as described previously (Jia et al., 2010). Four-week-old *DR5-GFP* reporter plants cultivated on WPM solid medium were carefully shifted to liquid WPM containing 0 mM (mock) or 200 mM NaCl (salt) and treated for 24 h. LR tips were detected afterward for the DR5-driving GFP fluorescence via a confocal microscope (Olympus FV1200). GFP was excited at 488 nm by an argon laser, and the emission was collected with a 505- to 530-nm bandpass filter. The fluorescence was quantified via the software FV10 ASW (Olympus).

Protein Stability Assay of IAA17.1

The constructs of *IAA17.1* and *IAA17.1m* fused with GFP were transiently transformed into the leaves of 4-week-old *Nicotiana benthamiana* via *A. tumefaciens*-mediated infiltration. The transformed *N. benthamiana* leaves were treated with auxin or salt for 2 h as follows: 50 μM CHX (mock treatment), 50 μM CHX and 20 μM IAA (auxin treatment), and 50 μM CHX and 200 mM NaCl (salt treatment). The nuclei of transfected epidermal cells were stained by DAPI (working solution, 1 μg mL^{-1}). Fluorescent signals of GFP and DAPI were documented using a confocal laser microscope (Olympus FV1200).

GFP fluorescence was viewed as described above. The DAPI signal was excited at 405 nm, and the emission was collected with a 450- to 480-nm bandpass filter.

Statistical Analyses

Quantitative data for expression analyses, GUS activities, fluorescence intensities, and physiological measurements were determined for statistical significance using Student's *t* test and one-way or two-way ANOVA as described in the corresponding figure legends. For ANOVA, Dunnett's test was performed to distinguish significant differences between pairwise samples (*, $P < 0.05$; **, $P < 0.01$; and ***, $P < 0.001$).

Accession Numbers

The sequences used in this study are available in Phytozome (version 11.0) under the following numbers: *miR390a* (MI0002305), *miR390b* (MI0002306),

miR390c (MI000230), *miR390d* (MI0002308), *ARF2.1* (Potri.012G106100.1), *ARF2.2* (Potri.015G105300.1), *ARF2.3* (Potri.002G207100.1), *ARF2.4* (Potri.001G066200.1) *ARF2.5* (Potri.003G163600.1), *ARF3.1* (Potri.004G050200.1), *ARF3.2* (Potri.011G059300.1), *ARF3.3* (Potri.011G059100.1), *ARF4* (Potri.009G011800.1), *IAA3.1* (Potri.005G053800.1), *IAA3.2* (Potri.013G041300.1), *GH3.2* (Potri.001G298300.1), *GH3.5* (Potri.001G410400.1), *PIN1a* (Potri.012G047200.1), *PIN1b* (Potri.015G038700.1), *PIN1c* (Potri.006G037000.1), and *PIN2* (Potri.018G139400.1).

Supplemental Data

The following supplemental materials are available.

Supplemental Figure S1. Sequence analysis and secondary structure prediction of poplar *miR390s*.

Supplemental Figure S2. Tissue-specific expression and promoter analyses of *miR390s* in poplar.

Supplemental Figure S3. Generation of *miR390*-OE and -STTM transgenic poplar lines.

Supplemental Figure S4. *miR390* target sites and *tasiARF*s harbored in the poplar *TAS3* genes.

Supplemental Figure S5. Phylogenetic analysis of ARF2/3/4 and the binding sites for *tasiARFs* within their transcripts.

Supplemental Figure S6. Expression levels of *tasiARFs* and *ARF2s* in *miR390*-OE and -STTM transgenic lines.

Supplemental Figure S7. Tissue-specific expression levels of *ARF3.1*, *ARF3.2*, and *ARF4* in poplar tissues determined by RT-qPCR.

Supplemental Figure S8. Overexpression of *ARF4* with disrupted binding sites of *tasiARFs* in the *miR390*-OE lines.

Supplemental Figure S9. Root phenotypes of *ARF4m*-OE and -RNAi transgenic seedlings exposed to mock and salt conditions.

Supplemental Figure S10. Nonnormalized data for root phenotypes of *ARF4m*-OE and -RNAi transgenic seedlings subjected to mock and salt conditions.

Supplemental Figure S11. Constitutive expression of *IAA17.1m* in the *miR390*-OE or *ARF4*-RNAi transgenic lines.

Supplemental Table S1. Sequences of oligonucleotide primers used in this study.

ACKNOWLEDGMENTS

We thank Dr. Bangjun Wang (Southwest University) for kindly providing the DR5-GFP plasmid.

Received October 31, 2017; accepted April 18, 2018; published May 1, 2018.

LITERATURE CITED

Adenot X, Elmayan T, Lauressergues D, Boutet S, Bouché N, Gasciolli V, Vaucheret H (2006) DRB4-dependent TAS3 trans-acting siRNAs control leaf morphology through AGO7. Curr Biol **16**: 927–932

Allen E, Xie Z, Gustafson AM, Carrington JC (2005) MicroRNA-directed phasing during trans-acting siRNA biogenesis in plants. Cell **121**: 207–221

Axtell MJ, Jan C, Rajagopalan R, Bartel DP (2006) A two-hit trigger for siRNA biogenesis in plants. Cell **127**: 565–577

Blilou I, Xu J, Wildwater M, Willemsen V, Paponov I, Friml J, Heidstra R, Aida M, Palme K, Scheres B (2005) The PIN auxin efflux facilitator network controls growth and patterning in Arabidopsis roots. Nature **433**: 39–44

Cabrera J, Barcala M, García A, Rio-Machín A, Medina C, Jaubert-Possamai S, Favery B, Maizel A, Ruiz-Ferrer V, Fenoll C, (2016) Differentially expressed small RNAs in Arabidopsis galls formed by *Meloidogyne javanica*: a functional role for miR390 and its TAS3-derived tasiRNAs. New Phytol **209**: 1625–1640

Chen S, Polle A (2010) Salinity tolerance of Populus. Plant Biol (Stuttg) **12**: 317–333

Chen S, Songkumarn P, Liu J, Wang GL (2009) A versatile zero background T-vector system for gene cloning and functional genomics. Plant Physiol **150**: 1111–1121

De Luis A, Markmann K, Cognat V, Holt DB, Charpentier M, Parniske M, Stougaard J, Voinnet O (2012) Two microRNAs linked to nodule infection and nitrogen-fixing ability in the legume *Lotus japonicus*. Plant Physiol **160**: 2137–2154

Dharmasiri N, Dharmasiri S, Weijers D, Lechner E, Yamada M, Hobbie L, Ehrismann JS, Jürgens G, Estelle M (2005) Plant development is regulated by a family of auxin receptor F box proteins. Dev Cell **9**: 109–119

Dickmann DI (2006) Silviculture and biology of short-rotation woody crops in temperate regions: then and now. Biomass Bioenergy **30**: 696–705

Duan L, Dietrich D, Ng CH, Chan PM, Bhalerao R, Bennett MJ, Dinneny JR (2013) Endodermal ABA signaling promotes lateral root quiescence during salt stress in *Arabidopsis* seedlings. Plant Cell **25**: 324–341

Dubrovsky JG, Sauer M, Napsucialy-Mendivil S, Ivanchenko MG, Friml J, Shishkova S, Celenza J, Benková E (2008) Auxin acts as a local morphogenetic trigger to specify lateral root founder cells. Proc Natl Acad Sci USA **105**: 8790–8794

Fahlgren N, Montgomery TA, Howell MD, Allen E, Dvorak SK, Alexander AL, Carrington JC (2006) Regulation of AUXIN RESPONSE FACTOR3 by TAS3 ta-siRNA affects developmental timing and patterning in Arabidopsis. Curr Biol **16**: 939–944

Friml J, Benková E, Blilou I, Wisniewska J, Hamann T, Ljung K, Woody S, Sandberg G, Scheres B, Jürgens G, (2002) AtPIN4 mediates sink-driven auxin gradients and root patterning in Arabidopsis. Cell **108**: 661–673

Galvan-Ampudia CS, Testerink C (2011) Salt stress signals shape the plant root. Curr Opin Plant Biol **14**: 296–302

Galvan-Ampudia CS, Julkowska MM, Darwish E, Gandullo J, Korver RA, Brunoud G, Haring MA, Munnik T, Vernoux T, Testerink C (2013) Halotropism is a response of plant roots to avoid a saline environment. Curr Biol **23**: 2044–2050

Garcia D, Collier SA, Byrne ME, Martienssen RA (2006) Specification of leaf polarity in Arabidopsis via the trans-acting siRNA pathway. Curr Biol **16**: 933–938

Geng Y, Wu R, Wee CW, Xie F, Wei X, Chan PM, Tham C, Duan L, Dinneny JR (2013) A spatio-temporal understanding of growth regulation during the salt stress response in *Arabidopsis*. Plant Cell **25**: 2132–2154

Gruber AR, Lorenz R, Bernhart SH, Neuböck R, Hofacker IL (2008) The Vienna RNA websuite. Nucleic Acids Res **36**: W70–W74

Guilfoyle TJ (1999) Auxin-regulated genes and promoters. *In* **PJJ Hooykaas, M Hall, KL Libbenga**, eds, Biochemistry and Molecular Biology of Plant Hormones. Elsevier, Leiden, The Netherlands, pp 423–459

Guilfoyle TJ, Hagen G (2007) Auxin response factors. Curr Opin Plant Biol **10**: 453–460

Hasegawa PM, Bressan RA, Zhu JK, Bohnert HJ (2000) Plant cellular and molecular responses to high salinity. Annu Rev Plant Physiol Plant Mol Biol **51**: 463–499

Hobecker KV, Reynoso MA, Bustos-Sanmamed P, Wen J, Mysore KS, Crespi M, Blanco FA, Zanetti ME (2017) The microRNA390/TAS3 pathway mediates symbiotic nodulation and lateral root growth. Plant Physiol **174**: 2469–2486

Iglesias MJ, Terrile MC, Windels D, Lombardo MC, Bartoli CG, Vazquez F, Estelle M, Casalongué CA (2014) MiR393 regulation of auxin signaling and redox-related components during acclimation to salinity in Arabidopsis. PLoS ONE **9**: e107678

Ji H, Pardo JM, Batelli G, Van Oosten MJ, Bressan RA, Li X (2013) The Salt Overly Sensitive (SOS) pathway: established and emerging roles. Mol Plant **6**: 275–286

Jia Z, Sun Y, Yuan L, Tian Q, Luo K (2010) The chitinase gene (Bbchit1) from *Beauveria bassiana* enhances resistance to *Cytospora chrysosperma* in *Populus tomentosa* Carr. Biotechnol Lett **32**: 1325–1332

Julkowska MM, Klei K, Fokkens L, Haring MA, Schranz ME, Testerink C (2016) Natural variation in rosette size under salt stress conditions corresponds to developmental differences between Arabidopsis accessions and allelic variation in the LRR-KISS gene. J Exp Bot **67**: 2127–2138

Kazan K (2013) Auxin and the integration of environmental signals into plant root development. Ann Bot **112**: 1655–1665

Ke Q, Kim HS, Wang Z, Ji CY, Jeong JC, Lee HS, Choi YI, Xu B, Deng X, Yun DJ, (2017) Down-regulation of GIGANTEA-like genes increases plant growth and salt stress tolerance in poplar. Plant Biotechnol J **15**: 331–343

Kepinski S, Leyser O (2005) The Arabidopsis F-box protein TIR1 is an auxin receptor. Nature **435**: 446–451

Li H, Tiwari SB, Hagen G, Guilfoyle TJ (2011) Identical amino acid substitutions in the repression domain of auxin/indole-3-acetic acid proteins have contrasting effects on auxin signaling. Plant Physiol **155**: 1252–1263

Li X, Lei M, Yan Z, Wang Q, Chen A, Sun J, Luo D, Wang Y (2014) The REL3-mediated TAS3 ta-siRNA pathway integrates auxin and ethylene signaling to regulate nodulation in Lotus japonicus. New Phytol **201**: 531–544

Liu B, Zhang J, Wang L, Li J, Zheng H, Chen J, Lu M (2014) A survey of Populus PIN-FORMED family genes reveals their diversified expression patterns. J Exp Bot **65**: 2437–2448

Liu W, Li RJ, Han TT, Cai W, Fu ZW, Lu YT (2015) Salt stress reduces root meristem size by nitric oxide-mediated modulation of auxin accumulation and signaling in Arabidopsis. Plant Physiol **168**: 343–356

Ludwig Y, Berendzen KW, Xu C, Piepho HP, Hochholdinger F (2014) Diversity of stability, localization, interaction and control of downstream gene activity in the maize Aux/IAA protein family. PLoS ONE **9**: e107346

Ma HS, Liang D, Shuai P, Xia XL, Yin WL (2010) The salt- and drought-inducible poplar GRAS protein SCL7 confers salt and drought tolerance in *Arabidopsis thaliana*. J Exp Bot **61**: 4011–4019

Marin E, Jouannet V, Herz A, Lokerse AS, Weijers D, Vaucheret H, Nussaume L, Crespi MD, Maizel A (2010) miR390, *Arabidopsis* TAS3 ta-siRNAs, and their AUXIN RESPONSE FACTOR targets define an autoregulatory network quantitatively regulating lateral root growth. Plant Cell **22**: 1104–1117

Munns R, Tester M (2008) Mechanisms of salinity tolerance. Annu Rev Plant Biol **59**: 651–681

Nagasaki H, Itoh J, Hayashi K, Hibara K, Satoh-Nagasawa N, Nosaka M, Mukouhata M, Ashikari M, Kitano H, Matsuoka M, (2007) The small interfering RNA production pathway is required for shoot meristem initiation in rice. Proc Natl Acad Sci USA **104**: 14867–14871

Nilsson J, Karlberg A, Antti H, Lopez-Vernaza M, Mellerowicz E, Perrot-Rechenmann C, Sandberg G, Bhalerao RP (2008) Dissecting the molecular basis of the regulation of wood formation by auxin in hybrid aspen. Plant Cell **20**: 843–855

Ottenschläger I, Wolff P, Wolverton C, Bhalerao RP, Sandberg G, Ishikawa H, Evans M, Palme K (2003) Gravity-regulated differential auxin transport from columella to lateral root cap cells. Proc Natl Acad Sci USA **100**: 2987–2991

Palme K, Gälweiler L (1999) PIN-pointing the molecular basis of auxin transport. Curr Opin Plant Biol **2**: 375–381

Paponov IA, Teale W, Lang D, Paponov M, Reski R, Rensing SA, Palme K (2009) The evolution of nuclear auxin signalling. BMC Evol Biol **9**: 126

Rouse D, Mackay P, Stirnberg P, Estelle M, Leyser O (1998) Changes in auxin response from mutations in an AUX/IAA gene. Science **279**: 1371–1373

Roy SJ, Negrão S, Tester M (2014) Salt resistant crop plants. Curr Opin Biotechnol **26**: 115–124

Sabatini S, Beis D, Wolkenfelt H, Murfett J, Guilfoyle T, Malamy J, Benfey P, Leyser O, Bechtold N, Weisbeek P, (1999) An auxin-dependent distal organizer of pattern and polarity in the Arabidopsis root. Cell **99**: 463–472

Si J, Zhou T, Bo W, Xu F, Wu R (2014) Genome-wide analysis of salt-responsive and novel microRNAs in *Populus euphratica* by deep sequencing. BMC Genet (Suppl 1) **15**: S6

Si-Ammour A, Windels D, Arn-Bouldoires E, Kutter C, Ailhas J, Meins F Jr, Vazquez F (2011) miR393 and secondary siRNAs regulate expression of the TIR1/AFB2 auxin receptor clade and auxin-related development of Arabidopsis leaves. Plant Physiol **157**: 683–691

Staswick PE, Serban B, Rowe M, Tiryaki I, Maldonado MT, Maldonado MC, Suza W (2005) Characterization of an *Arabidopsis* enzyme family that conjugates amino acids to indole-3-acetic acid. Plant Cell **17**: 616–627

Sun F, Zhang W, Hu H, Li B, Wang Y, Zhao Y, Li K, Liu M, Li X (2008) Salt modulates gravity signaling pathway to regulate growth direction of primary roots in Arabidopsis. Plant Physiol **146**: 178–188

Tamura K, Stecher G, Peterson D, Filipski A, Kumar S (2013) MEGA6: Molecular Evolutionary Genetics Analysis version 6.0. Mol Biol Evol **30**: 2725–2729

Tan X, Calderon-Villalobos LI, Sharon M, Zheng C, Robinson CV, Estelle M, Zheng N (2007) Mechanism of auxin perception by the TIR1 ubiquitin ligase. Nature **446**: 640–645

Tang RJ, Liu H, Bao Y, Lv QD, Yang L, Zhang HX (2010) The woody plant poplar has a functionally conserved salt overly sensitive pathway in response to salinity stress. Plant Mol Biol **74**: 367–380

Vanneste S, Friml J (2009) Auxin: a trigger for change in plant development. Cell **136**: 1005–1016

Varkonyi-Gasic E, Wu R, Wood M, Walton EF, Hellens RP (2007) Protocol: a highly sensitive RT-PCR method for detection and quantification of microRNAs. Plant Methods **3**: 12

von Behrens I, Komatsu M, Zhang Y, Berendzen KW, Niu X, Sakai H, Taramino G, Hochholdinger F (2011) Rootless with undetectable meristem 1 encodes a monocot-specific AUX/IAA protein that controls embryonic seminal and post-embryonic lateral root initiation in maize. Plant J **66**: 341–353

Wang Y, Zhang W, Li K, Sun F, Han C, Wang Y, Li X (2008) Salt-induced plasticity of root hair development is caused by ion disequilibrium in *Arabidopsis thaliana*. J Plant Res **121**: 87–96

Wang Y, Li K, Li X (2009) Auxin redistribution modulates plastic development of root system architecture under salt stress in *Arabidopsis thaliana*. J Plant Physiol **166**: 1637–1645

Wesley SV, Helliwell CA, Smith NA, Wang MB, Rouse DT, Liu Q, Gooding PS, Singh SP, Abbott D, Stoutjesdijk PA, (2001) Construct design for efficient, effective and high-throughput gene silencing in plants. Plant J **27**: 581–590

West G, Inzé D, Beemster GTS (2004) Cell cycle modulation in the response of the primary root of Arabidopsis to salt stress. Plant Physiol **135**: 1050–1058

Worley CK, Zenser N, Ramos J, Rouse D, Leyser O, Theologis A, Callis J (2000) Degradation of Aux/IAA proteins is essential for normal auxin signalling. Plant J **21**: 553–562

Xia R, Xu J, Meyers BC (2017) The emergence, evolution, and diversification of the miR390-TAS3-ARF pathway in land plants. Plant Cell **29**: 1232–1247

Xie Z, Allen E, Wilken A, Carrington JC (2005) DICER-LIKE 4 functions in trans-acting small interfering RNA biogenesis and vegetative phase change in *Arabidopsis thaliana*. Proc Natl Acad Sci USA **102**: 12984–12989

Yan J, Gu Y, Jia X, Kang W, Pan S, Tang X, Chen X, Tang G (2012) Effective small RNA destruction by the expression of a short tandem target mimic in *Arabidopsis*. Plant Cell **24**: 415–427

Yang Y, Tang RJ, Jiang CM, Li B, Kang T, Liu H, Zhao N, Ma XJ, Yang L, Chen SL, (2015) Overexpression of the PtSOS2 gene improves tolerance to salt stress in transgenic poplar plants. Plant Biotechnol J **13**: 962–973

Yao W, Wang S, Zhou B, Jiang T (2016) Transgenic poplar overexpressing the endogenous transcription factor ERF76 gene improves salinity tolerance. Tree Physiol **36**: 896–908

Yifhar T, Pekker I, Peled D, Friedlander G, Pistunov A, Sabban M, Wachsman G, Alvarez JP, Amsellem Z, Eshed Y (2012) Failure of the tomato trans-acting short interfering RNA program to regulate AUXIN RESPONSE FACTOR3 and ARF4 underlies the wiry leaf syndrome. Plant Cell **24**: 3575–3589

Yin Z, Han X, Li Y, Wang J, Wang D, Wang S, Fu X, Ye W (2017) Comparative analysis of cotton small RNAs and their target genes in response to salt stress. Genes (Basel) **8**: E369

Yoon EK, Yang JH, Lim J, Kim SH, Kim SK, Lee WS (2010) Auxin regulation of the microRNA390-dependent transacting small interfering RNA pathway in Arabidopsis lateral root development. Nucleic Acids Res **38**: 1382–1391

Yu LH, Wu SJ, Peng YS, Liu RN, Chen X, Zhao P, Xu P, Zhu JB, Jiao GL, Pei Y, (2016) Arabidopsis EDT1/HDG11 improves drought and salt tolerance in cotton and poplar and increases cotton yield in the field. Plant Biotechnol J **14**: 72–84

Zhang JL, Shi H (2013) Physiological and molecular mechanisms of plant salt tolerance. Photosynth Res **115**: 1–22

Zhao H, Jiang J, Li K, Liu G (2017) Populus simonii × Populus nigra WRKY70 is involved in salt stress and leaf blight disease responses. Tree Physiol **37**: 827–844

Zhao Y, Wang T, Zhang W, Li X (2011) SOS3 mediates lateral root development under low salt stress through regulation of auxin redistribution and maxima in Arabidopsis. New Phytol **189**: 1122–1134

Zhou C, Han L, Fu C, Wen J, Cheng X, Nakashima J, Ma J, Tang Y, Tan Y, Tadege M, (2013) The trans-acting short interfering RNA3 pathway and no apical meristem antagonistically regulate leaf margin development and lateral organ separation, as revealed by analysis of an argonaute7/lobed leaflet1 mutant in *Medicago truncatula*. Plant Cell **25**: 4845–4862